NSWC TR 87-200

PHASE RELATIONSHIPS IN HIGH TEMPERATURE CERAMICS

BY R. P. TURCOTTE (FLOW RESEARCH COMPANY)

FOR NAVAL SURFACE WEAPONS CENTER
STRATEGIC SYSTEMS DEPARTMENT

APRIL 1987

NAVAL SURFACE WEAPONS CENTER

Dahlgren, Virginia 22448-5000 • Silver Spring, Maryland 20903-5000

REPORT DOCUMENTATION PAGE

1a REPORT SECURITY CLASSIFICATION UNCLASSIFIED	1b RESTRICTIVE MARKINGS
2a SECURITY CLASSIFICATION AUTHORITY	3 DISTRIBUTION / AVAILABILITY OF REPORT Approved for public release; distribution is unlimited.
2b DECLASSIFICATION / DOWNGRADING SCHEDULE	
4 PERFORMING ORGANIZATION REPORT NUMBER(S) Flow TR 409	5 MONITORING ORGANIZATION REPORT NUMBER(S) NSWC TR 87-200
6a NAME OF PERFORMING ORGANIZATION Flow Research Company 6b OFFICE SYMBOL (If applicable)	7a NAME OF MONITORING ORGANIZATION Naval Surface Weapons Center (K20)
6c ADDRESS (City, State, and ZIP Code) 21414 68th Avenue South Kent, WA 98032	7b ADDRESS (City, State, and ZIP Code) 10901 New Hampshire Avenue Silver Spring, MD 20903-5000
8a NAME OF FUNDING / SPONSORING ORGANIZATION 8b OFFICE SYMBOL (If applicable)	9 PROCUREMENT INSTRUMENT IDENTIFICATION NUMBER N60921-86-C-0270
8c ADDRESS (City, State, and ZIP Code)	10 SOURCE OF FUNDING NUMBERS PROGRAM ELEMENT NO. / PROJECT NO. / TASK NO / WORK UNIT ACCESSION NO.

11 TITLE (Include Security Classification)
Phase Relationships in High Temperature Ceramics

12 PERSONAL AUTHOR(S)
R. P. Turcotte

13a TYPE OF REPORT	13b TIME COVERED	14 DATE OF REPORT (Year, Month, Day)	15 PAGE COUNT
Phase I Final Report	FROM _____ TO _____	1987, April	41

16 SUPPLEMENTARY NOTATION

17 COSATI CODES			18 SUBJECT TERMS (Continue on reverse if necessary and identify by block number)
FIELD	GROUP	SUB-GROUP	Ceramics, Solubility, Phase Diagram
11	02	01	

19 ABSTRACT (Continue on reverse if necessary and identify by block number)

The objective of this work was to establish an efficient means of determining the high temperature phase behavior of the HfO_2-Ta_2O_5 system under conditions of relevance to their potential use in propulsion sytem environments. A primary objective was to establish melting temperatures for the mixed oxides and to identify phases formed in the high temperature portions of the phase diagram, above 2500°F (1400°C). The approaches evaluated included traditional anneal quench studies and use of CO_2 laser heating in controlled atmospheres. Melting points were measured using an optical pyrometer/laser fusion approach. Phases formed were characterized primarily by x-ray diffraction and electron microscopy. The liquidous curve for the oxide system has been established and two new phases identified for the oxide system.

20 DISTRIBUTION / AVAILABILITY OF ABSTRACT	21 ABSTRACT SECURITY CLASSIFICATION
☒ UNCLASSIFIED/UNLIMITED ☐ SAME AS RPT. ☐ DTIC USERS	UNCLASSIFIED
22a NAME OF RESPONSIBLE INDIVIDUAL Mark Opeka	22b TELEPHONE (Include Area Code) (301) 394-3513 / 22c OFFICE SYMBOL K20

DD FORM 1473, 84 MAR 83 APR edition may be used until exhausted
All other editions are obsolete

★U.S. Government Printing Office: 1985—539-012

FOREWORD

The work described in this report is the result of Phase I Small Business Innovation Research (SBIR) contract funded through the Naval Surface Weapons Center (NSWC), White Oak Laboratory. Mr. Mark Opeka of NSWC was the technical monitor for the project and contributed to its direction.

A number of colleagues in the Advanced Materials Division of Flow Research Company contributed directly to the successful outcome of the study. Glen Moore helped with equipment setup, x-ray, and SEM work. Ender Savrun helped with the carbide work. Art Day designed the environmental chamber/furnace and helped with the laser setup/ pyrometry. Brian Walker helped with the laser studies. Birol Sonuparlak provided a critical technical review of the work. Julie Upton and Carole Dennis organized and typed the final report.

Approved by:

D. B. COLBY, Head
Strategic Systems Department

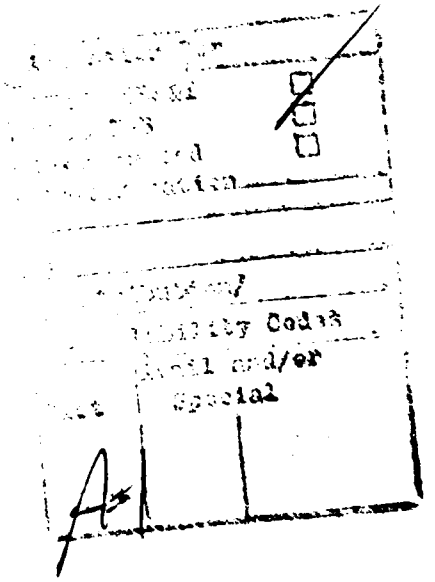

CONTENTS

ILLUSTRATIONS

ILLUSTRATIONS (Cont.)

TABLES

INTRODUCTION

This report describes results of a Small Business Innovation Research (SBIR) Phase I study of high temperature ceramic systems which could find applications as components in propulsion applications. Since desired use temperatures extend to temperatures as high as 5000°F, there are relatively few materials which are attractive. Thus, carbides and oxides of hafnium, zirconium and tantalum, as well as a few other high melting point ceramics like ThO_2,are potentially useful. For a variety of reasons certain binary compounds may be desirable, as might be additions of other dopants (e.g., B_2O_3). Unfortunately, very little information is available concerning the high temperature properties of binary and ternary systems of interest. The objective of this work was to establish an efficient means of determining the high temperature phase behavior of such systems under conditions of relevance to their potential use in propulsion system environments. This initial Phase I effort involved study of two related systems, HfO_2/Ta_2O_5 and HfC/TaC with a primary emphasis on the oxides, for which only very limited information has been published. A primary objective was to establish melting temperatures for the mixed oxides and to identify phases formed in the high temperature portions of the phase diagram, above 2500°F (1400°C).

The approaches evaluated included traditional anneal quench studies and use of CO_2 laser heating in controlled atmospheres. Melting points were measured using an optical pyrometer/laser fusion approach. Phases formed were characterized primarily by x-ray diffraction and electron microscopy. The liquidous curve for the oxide system has been established and two new phases identified for the oxide system. A limited effort on the related carbides will be reported later. Unless otherwise noted all of the work was conducted in air.

EXPERIMENTAL

MATERIALS

Starting materials were purchased from Cerac, Inc., with certificates of analysis. X-ray diffraction analysis of all four materials agreed with Powder Diffraction File (PDF) standards with no indication of impurity phases.

Ta_2O_5 (T-1013) lot #7830, 325 mesh, 99.95% pure, major impurities (PPM) as follows:

Nb less than 50
Mo less than 10
W less than 10
Si less than 10

HfO_2 (H-1011) lot #7854, 325 mesh, 99.95% pure, major impurities (PPM) as follows:

Zr 1.1%
Sr less than 100
Na less than 100
Zn less than 50

Starting materials were dried at 150°C in quartz crucibles then weighed (+/- 0.1 mg) to give desired mixed compositions. The various compositions were mixed by forming an alcohol slurry, dried and pressed to form pellets 1 cm in diameter x 2 mm thick. The pellets were then heat treated as discussed in the "Results" section. The following compositions were prepared, primarily based on a literature review of related oxide systems which suggested certain compounds might form in the system.

Hf/Ta atom ratio = 20, 10, 6, 4, 2.5, 2, 1, 0.25, 0.167, 0.05

EQUIPMENT

X-Ray Diffraction - Three different diffactometers were used depending on availability, including Philips (University of Washington), Siemens (Scan Tech, Inc.) and Philips (AMD equipment). In all cases, copper radiation was used. Traces were generally recorded at 1° 2θ/minute on strip chart recorders.

Laser - Photon Sources, Model 305, 500 Watt, TEM_{oo} mode. In all of the work to be discussed, the laser was operated in the continuous mode rather than pulsed. Although some experiments involved use of a lens to focus the beam, virtually all of the results used the unfocused beam directly, heating the materials from above. The spot size was approximately 0.5 cm^2 and slightly oval shaped based on burn patterns. A chopper was placed in the beam to reduce intensity by a factor of two to four. Power levels were manually set with a ten turn (digital) potentiometer. The typical power levels required in this study ranged from 10 watts to over 500 watts. The laser was upgraded to provide very stable power/beam intensity. We found materials could be reproducibly heated to the same constant temperature over tens of minutes, although this was not really required for the present application.

It is possible to estimate the temperature of a sample heated under a laser beam by considering the energy balance in equilibrium. Energy flows into the sample by absorption of radiation (infrared light) from the laser beam. Energy is lost from the sample by thermal conduction into surrounding contacting materials and also by reradiation. When the sample has reached an equilibrium temperature, the flow of energy into the sample must equal the energy losses to the surroundings. Thermal conductivity losses can be minimized by heating the sample in vacuum on a low thermal conductivity support such as fibrous zirconia. The radiated energy loss can be estimated from Plank's blackbody radiation law and the known sample emissivity. If the sample is spherical with a diameter on the order of the laser beam diameter, then nearly all of the energy of the laser beam bill be absorbed. Equating the absorbed energy with the radiated energy and assuming a typical emissivity value of 0.77 yields the temperature vs. diameter curve shown in Figure 1. The temperature rises rapidly as the sample size (and focused beam size) decreases. It should thus be possible to melt any known material with only moderate focusing of the subject laser. This result has been experimentally verified by easily reaching temperatures above 3000°C with the unfocused beam.

The melting studies involved use of small beads, abut 1 to 1.5mm in diameter, assuming the small interface region between two contacting beads was at a constant temperature. Certainly there was some temperature gradient (depending on orientation, heat conduction, etc.),

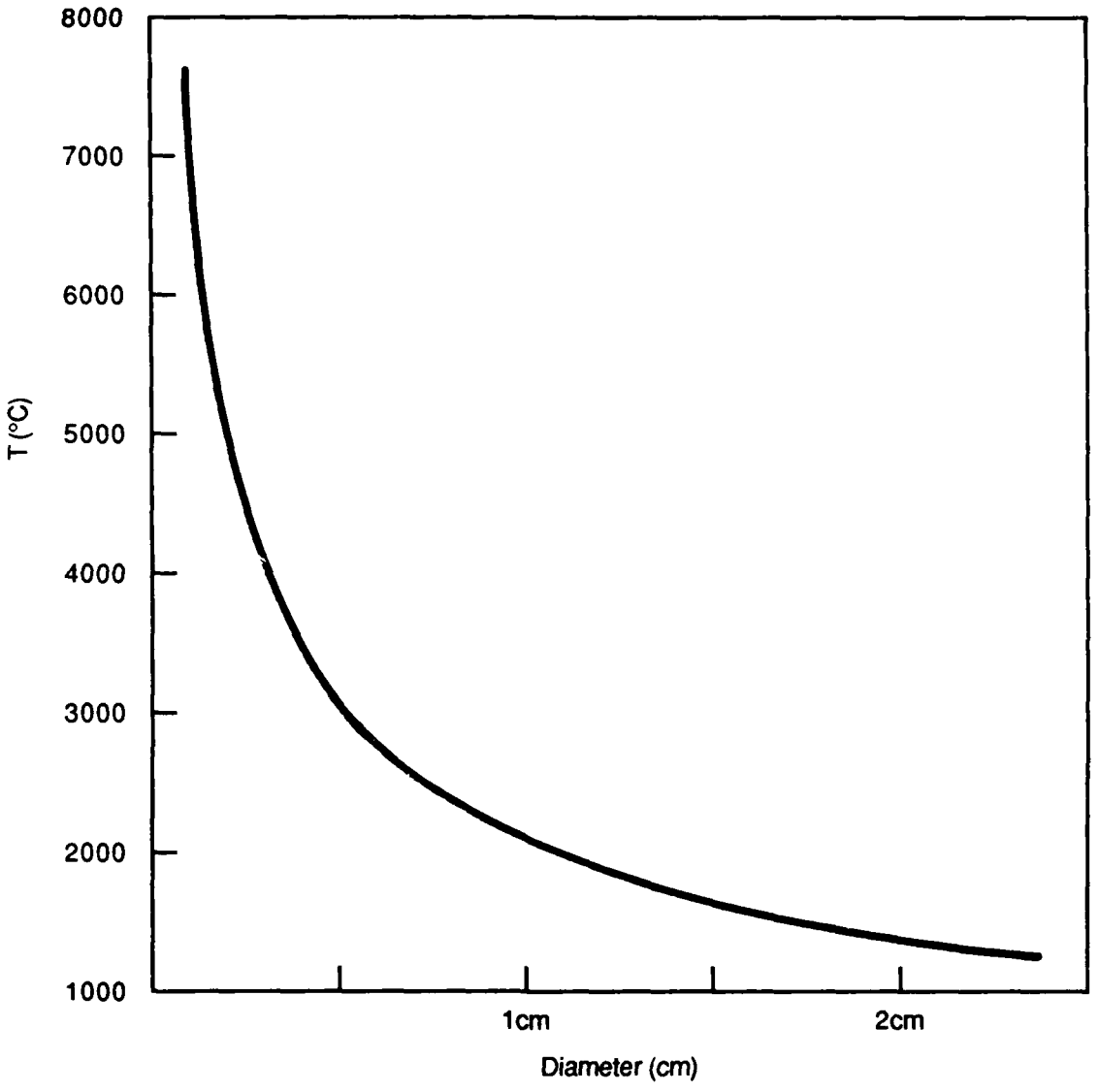

FIGURE 1. MAXIMUM LASER HEATED SURFACE TEMPERATURE VERSUS BEAM DIAMETER FOR A 500 WATT LASER

but burn patterns in plastic suggested the center $1mm^2$ of the beam was at a nearly flat photon density. The temperature profile was measured on the surface of a low density plate of HfO_2 as a possible worst case situation. This showed temperatures dropping by almost 100^oC per millimeter from the center, at a temperature of 1800^oC and about 90^oC per millimeter at 2200^oC.

Filament Furnace/Environmental Chamber - A filament vacuum furnace was constructed for use on this project, which also served as a controlled environment chamber in the laser heating experiments. A schematic of the furnace is shown in Figure 2. Small samples could be heated to as high as 2500^oC with tantalum heaters.

With regard to using the chamber with the laser, considerable problems were encountered with destruction of both ZnSe and NaCl windows. Two focusing lenses (Ge and ZnSe) were also destroyed during the course of the project.

Optical Pyrometer - A commercial Land-Minolta optical pyrometer, Cyclops Model 52, was used to measure melting temperatures. This pyrometer has digital readout and automatic emissivity correction features. As discussed in the results section, an emissivity setting of 1.0 and the definition of "melting" as formation of a liquid "neck" between contacting beads gave melting point temperatures for pure Ta_2O_5 and pure HfO_2 in close agreement with the accepted values. Therefore, the data obtained for the mixed oxide compositions are in effect accurate, through direct calibration based on the end member oxides. In general, the reliability and repeatability of the pyrometer readings were observed to be within +/- 10^oC. Other far more subjective factors discussed later lead to much larger uncertainties in the melting point data.

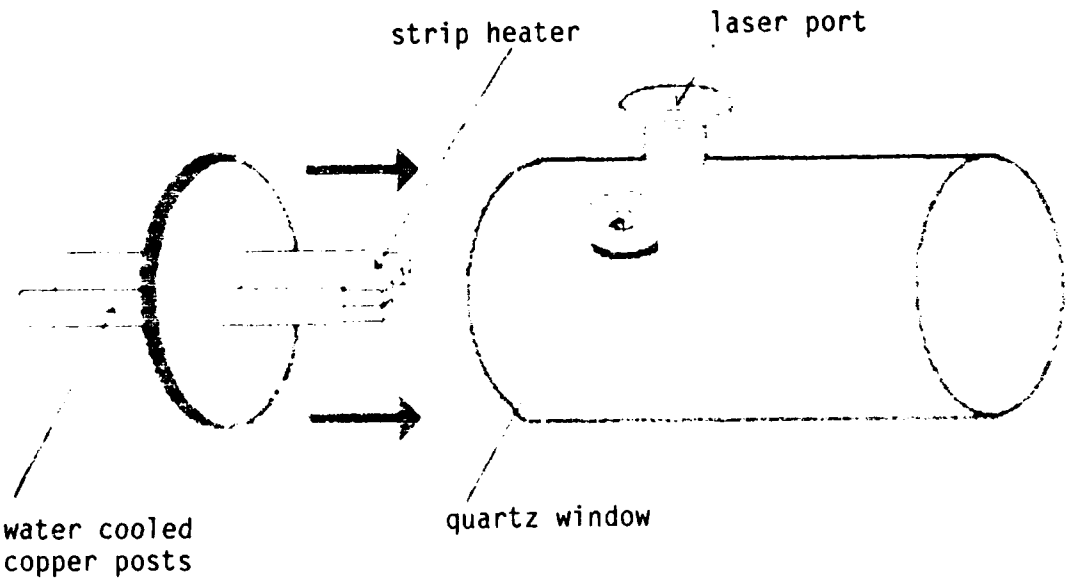

FIGURE 2. SCHEMATIC OF FILAMENT FURNACE/ LASER ENVIRONMENTAL CHAMBER

Electron Microscopy - A Hitachi Scanning Electron Microscope (Model 570), equipped with energy dispersive x-ray analysis features (Kevex, Model 8005) was used to examine the micro-structures and compositions of the materials studied.

DTA - A commercial Perkin-Elmer DTA/DSC was used with argon cover gas at heating rates of 10°C/min. The system was used in the DSC mode and calibrated to the correct melting point for gold (1063°C).

RESULTS and DISCUSSION

MELTING POINT DETERMINATION

Melting points for the mixed oxides were determined by visual observation of millimeter sized beads as the laser intensity was manually increased, in steps giving temperature rises of about 20°C. Initial experiments were conducted to determine the most desirable physical form of the material to evaluate, including various irregular and regular shapes, low vs. high density solids, means of support, etc. An equally difficult question was what to use for emissivity corrections and what definition to apply as identifying the "melting point." It was found that very regular 1-2 millimeter diameter beads

could readily be formed by melting irregular shapes on a large graphite block. Because of its high thermal conductivity, a block 12" in diameter and 6" thick requires 15 minutes or more of direct full power heating before being hot to the touch. Hence, graphite was used to support the materials of interest.

A large number of millimeter size beads of each composition were prepared. A standard arrangement of one bead resting on three beads (or two resting on five or six) was found to give reproducible "melting points" for both Ta_2O_5 and HfO_2 with the pyrometer emissivity set at 1.0. "Melting" was defined as the formation of a liquid "neck" between two adjacent beads, positioned in the beam to give a uniform temperature at the interface. The temperature sensing area, visible as a circle in the pyrometer eyepiece, was smaller than the individual bead whose temperature was being followed as the laser power was increased. The pyrometer was mounted on a tripod and a lens with a 10" focal length was used. Because the beads were originally quenched from the melt, care was taken to gradually increase temperature, giving the material time to approach equilibrium as the melting temperature was approached. An individual melting point was nevertheless determined quite rapidly, within 5-10 minutes. Because the geometry was slightly different in each experiment and adjacent spheres could be at slightly different temperatures, etc., it is easy to recognize that this approach gives rise to considerable scatter as evidenced by the final results, which are shown in Figure 3. The compositions rich in Ta_2O_5 were easier to evaluate since at the melting point, the entire bead would collapse, in contrast to the high hafnia compositions where the beads remained largely solid. It is clear from the figure that the high melting point advantage for pure HfO_2 rapidly falls off with addition of Ta_2O_5. On that basis alone, it would appear mixed oxides should contain less than 5 mole % Ta_2O_5 for very high temperature applications. The melting point curve for compositions up to 66 mole % HfO_2 is very flat, falling within the range of 1800-2200°C. The data are plotted showing the average value of four or more individual measurements for each composition. The bars drawn represent the observed scatter band. Note the measured average melting point values were 1903°C for Ta_2O_5 and 2822°C for HfO_2, in reasonable agreement with literature values of 1887°C and 2800-2900°C respectively.

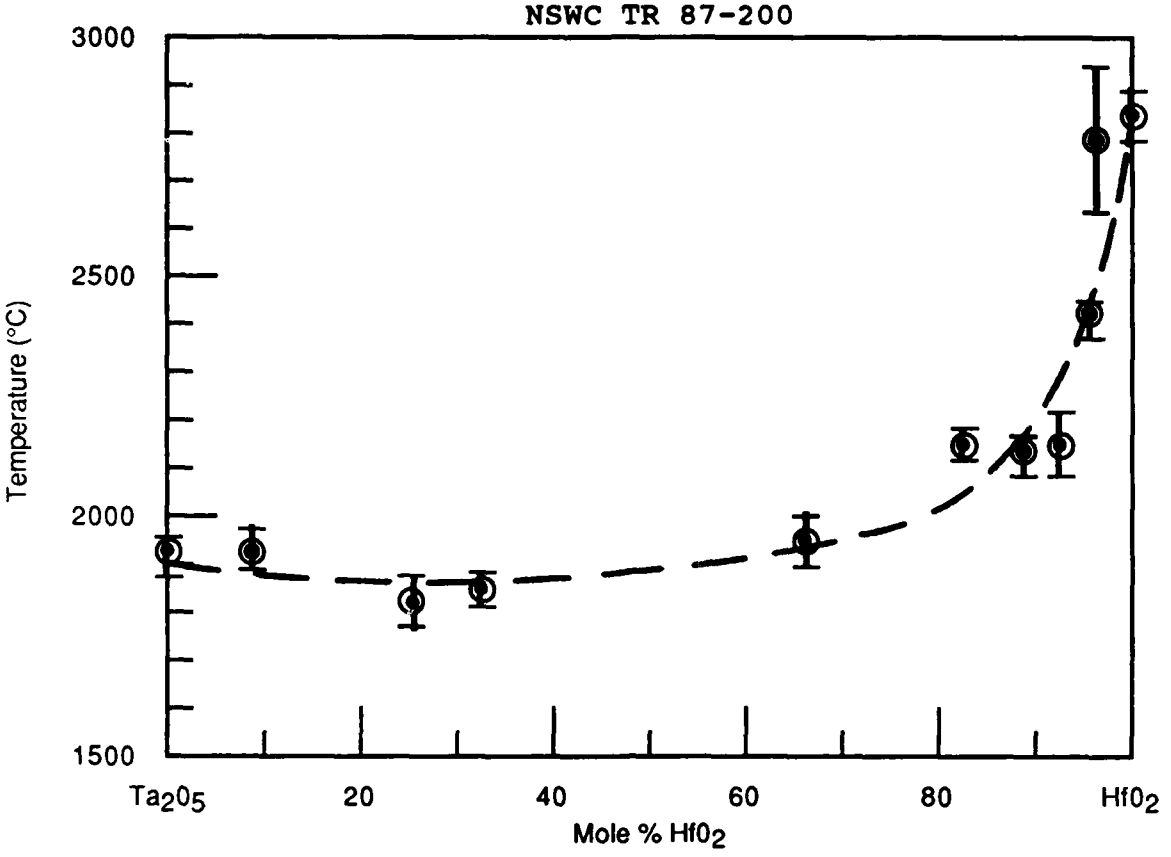

FIGURE 3. MELTING POINTS FOR MIXED HfO_2/Ta_2O_5 OXIDES

PHASE BEHAVIOR STUDIES

A series of initial experiments was undertaken to determine whether the pure oxides were sufficiently reactive that simple mixing and pressing into pellets followed by a high temperature treatment could give results which might be taken as near the equilibrium condition. The very high cost and 90-day delivery time for alkoxides of these elements precluded using a molecular mixing approach which would be most desirable. Although it was determined that tantalum oxide is entirely consumed in reaction with HfO_2 after a few minutes heating at 1500°C, the results of the study are sufficiently complex that this issue should be reconsidered in further studies. In any case, various series of heat treated samples of the mixed oxide compositions were studied involving: 1) melt quenching, 2) 1900°C quench, 3) 1500°C, 20°C/minute cooldown, 5) diffusion couple samples, 6) volatility, 7) differential thermal analysis. Series 1 and 2 were prepared using laser heating. For series 2, pellets which had previously been heated to 1500°C for several hours were subjected to surface heating at about 1900°C. For series 3, pellets of the mixed oxide composition were heated at 400°C/hr to 1500°C, held one hour and then physically removed (alumina crucibles were used). For series 4, samples were heated to 1500°C at 100°C/hr and cooled at 20°C/minute to 700°C, at which temperature they were removed from the furnace.

An additional attempted heat treatment to 1700°C resulted in extensive reaction of the materials (especially high Ta_2O_5 compositions) with the alumina crucible. These were not analyzed.

The results of the phase formation study at this point cannot be entirely interpreted, partly because we have emphasized temperatures above 1500°C, whereas all of the work reported on related studies really is representative of lower temperatures below 1500°C. The review of previous work suggested possible formation of a number of compounds, as shown in Figure 4. The compositions of these phases naturally led to the choice of compositions chosen for study in the program. Our study has identified a new phase which occurs in quenched liquids and the phase with composition $2HfO_2 \cdot Ta_2O_5$ ($Hf_2Ta_2O_9$) is shown to be especially important as a phase boundary. It should be noted in Figure 4 that there is no information actually available concerning the temperature range of stability for the various compounds identified. Figure 5 shows diffraction patterns for some of the key phases in the system which will allow the reader to better understand the actual x-ray diffraction traces presented later. It should be clear from Figure 5 that patterns resulting from mixtures of phases in the system can be very challenging to separate because of the overlapping of many reflections. This difficulty is further compounded with regard to elemental analysis of crystallites using the electron microscope because of all the fluorescence peaks for Hf and Ta are strongly overlapped. A resolution to most of these analytical difficulties has been achieved in the initial study, but additional work is needed to understand the solid state structures.

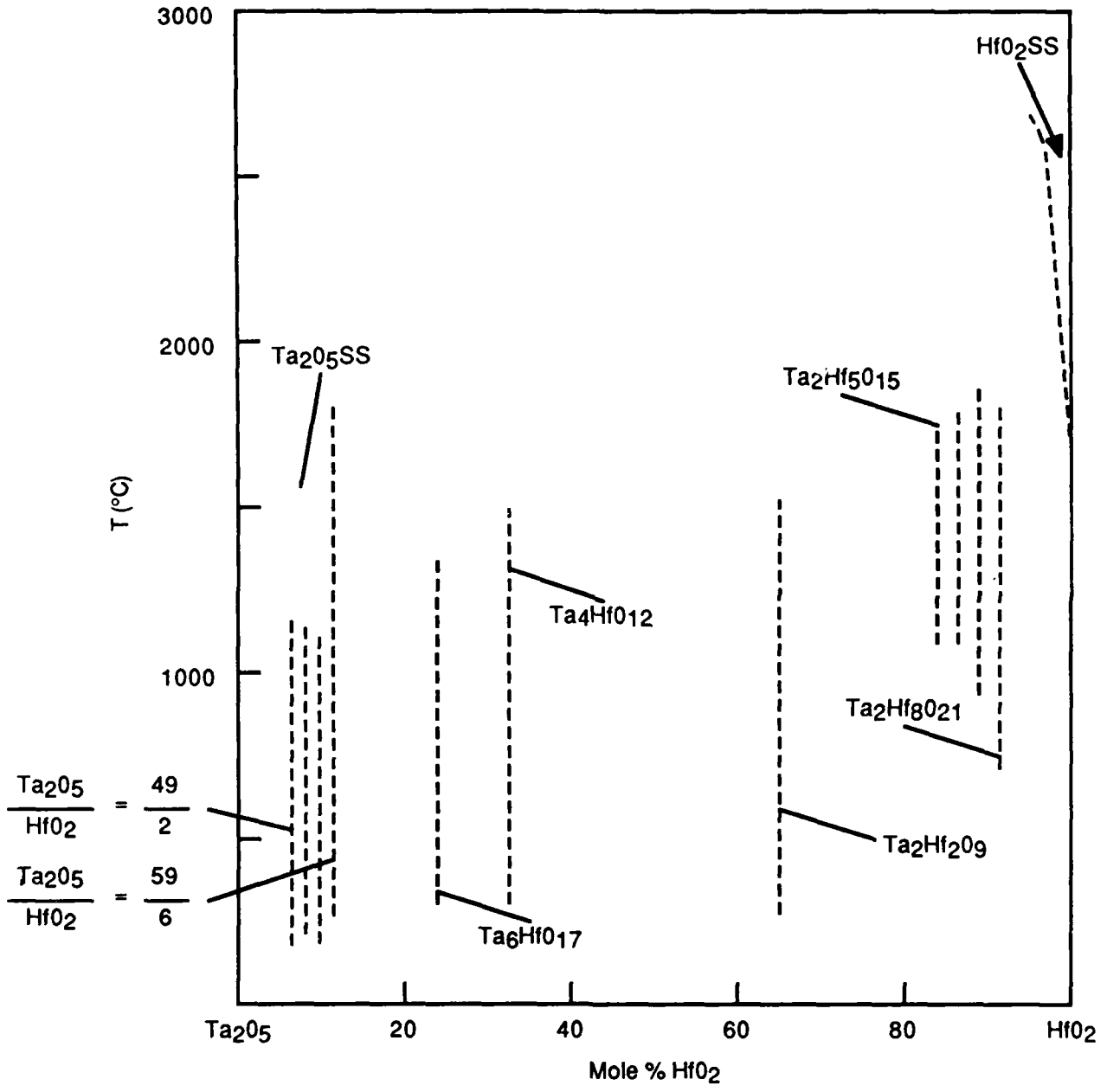

FIGURE 4. **HYPOTHETICAL PHASES IN THE HfO_2-Ta_2O_5 System**

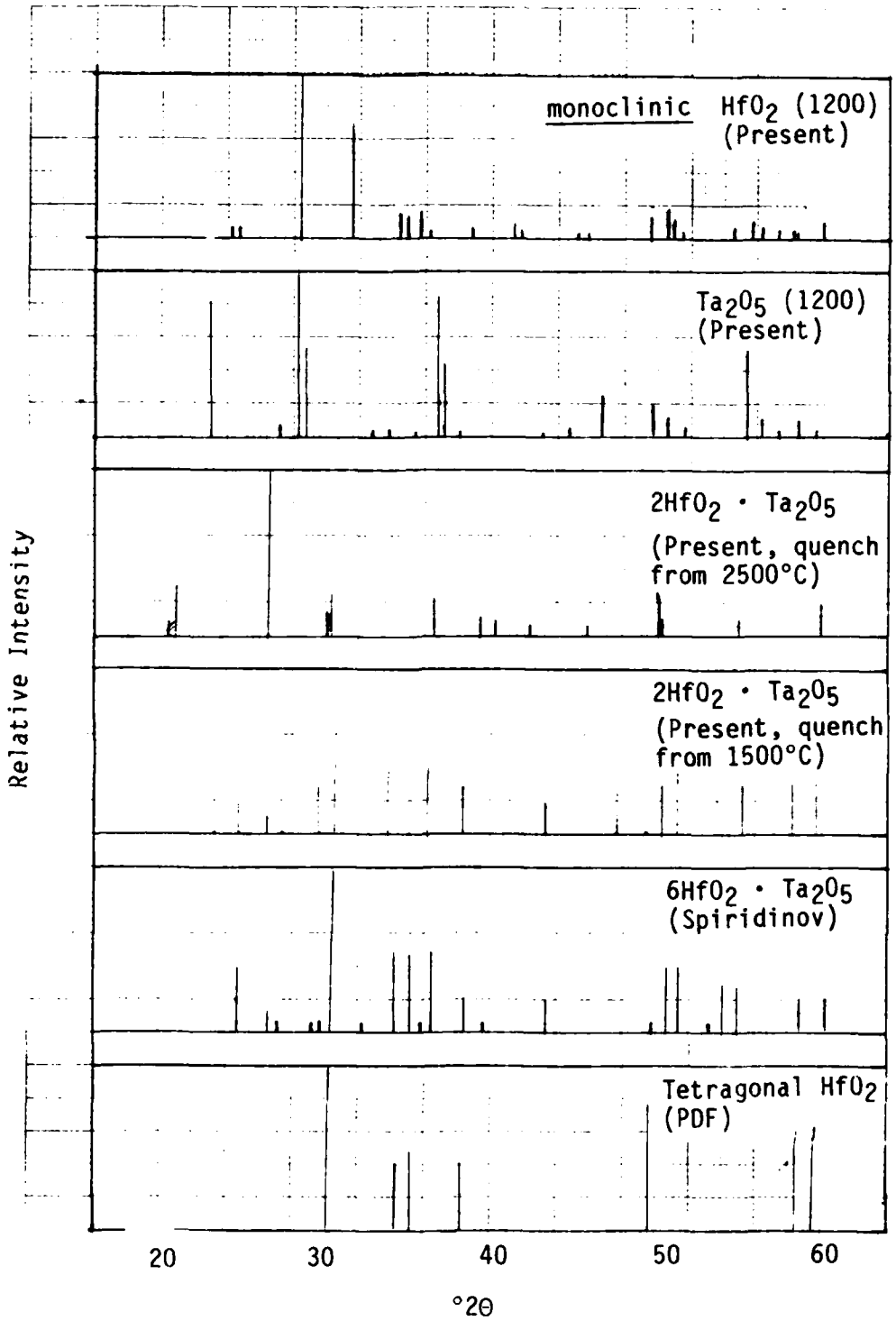

FIGURE 5. X-RAY DIFFRACTION PATTERNS OF KEY PHASES

Melt Quenching

Beads of molten oxides were quenched from 2000°C or higher and studied by x-ray diffraction and by electron microscopy. Additional samples of larger surface areas were prepared by surface melting portions of pressed pellets to improve x-ray diffraction sensitivity. These were polished to ensure the data represented the bulk liquid rather than the immediate surface.

X-Ray Diffraction - Traces are shown in Figure 6. They are immediately striking because the two strongest reflections (and many others) occur for every composition. It may be noted that several of the samples studied (Hf/Ta = 2.5, 10, 6) had small surface areas compared to the others and required using higher sensitivity. The broad band near 25° 2θ for the 2.5 ratio composition is from the mounting clay used to support the sample. In any case, it appears that mainly one phase is present from Hf/Ta = 20 to Hf/Ta = 1, whereas the remaining high Ta compositions contain at least two major phases. These patterns have not been indexed yet.

Electron Microscopy - Electron Microscopy of the liquid quenched materials was also very interesting, but does not correlate well to the above XRD results. Representative micrographs are shown in Figure 7. Five of the eight mixed oxides showed some form of two-phase structure, mainly as an obvious residual frozen liquid seen in higher volume fraction for intermediate compositions like Hf/Ta = 2.5 and much less at high Hf or very high Ta compositions. As will be discussed, this residual liquid phase is rich in Ta compared to the primary phase. Most of the quenched samples also contained considerable large porosity, concentrated toward the center of the beads. This was expected since the volume change on melting ceramics is often more than 5%. As the beads solidify from the outside-inward, some porosity must develop.

The quantitative analysis of Hf and Ta with the energy dispersive spectrometer (EDS) equipment is not easy because these elements are adjacent in the periodic table (atomic number 72 and 73) and their x-ray fluorescence characteristic spectra overlap extensively. Figures 8 and 9 show typical spectra. For Figure 8, the atomic ratio was Hf/Ta=6.0. For Figure 9, the ratio was Hf/Ta= 0.17 or Ta/Hf = 5.9. It is evident that the software does a good job of identifying the various fluorescence peaks, but they are not resolved. We were nevertheless able to to calibrate the equipment to allow fairly accurate elemental analysis. The L series lines in the region 7 to 10.1 keV were used. The Kevex software automatically goes through a curve fitting process to generate apparent concentrations. By using all of the fluorescence coming from a general area view (rather than a spot

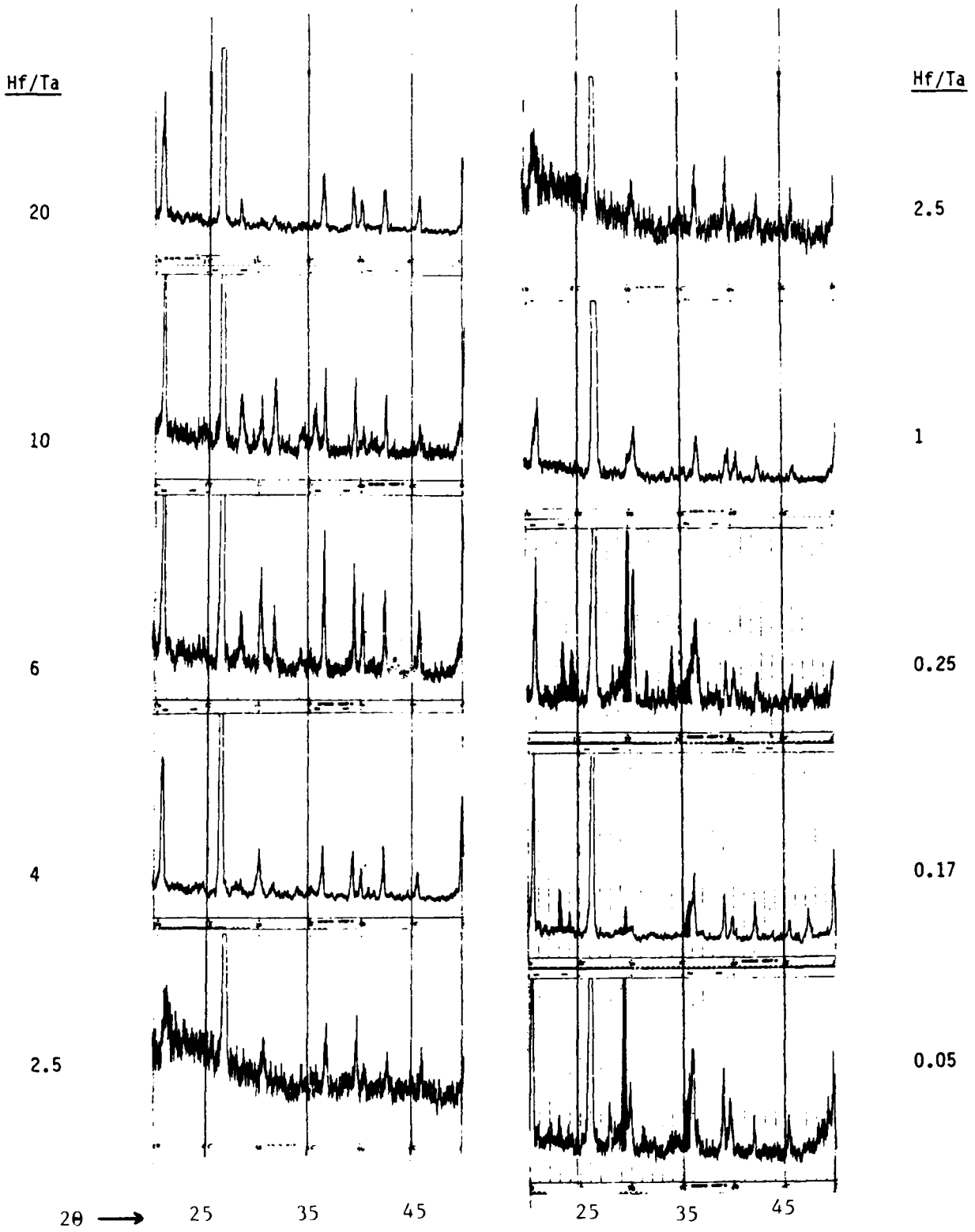

FIGURE 6. X-RAY PATTERNS OF QUENCHED LIQUIDS

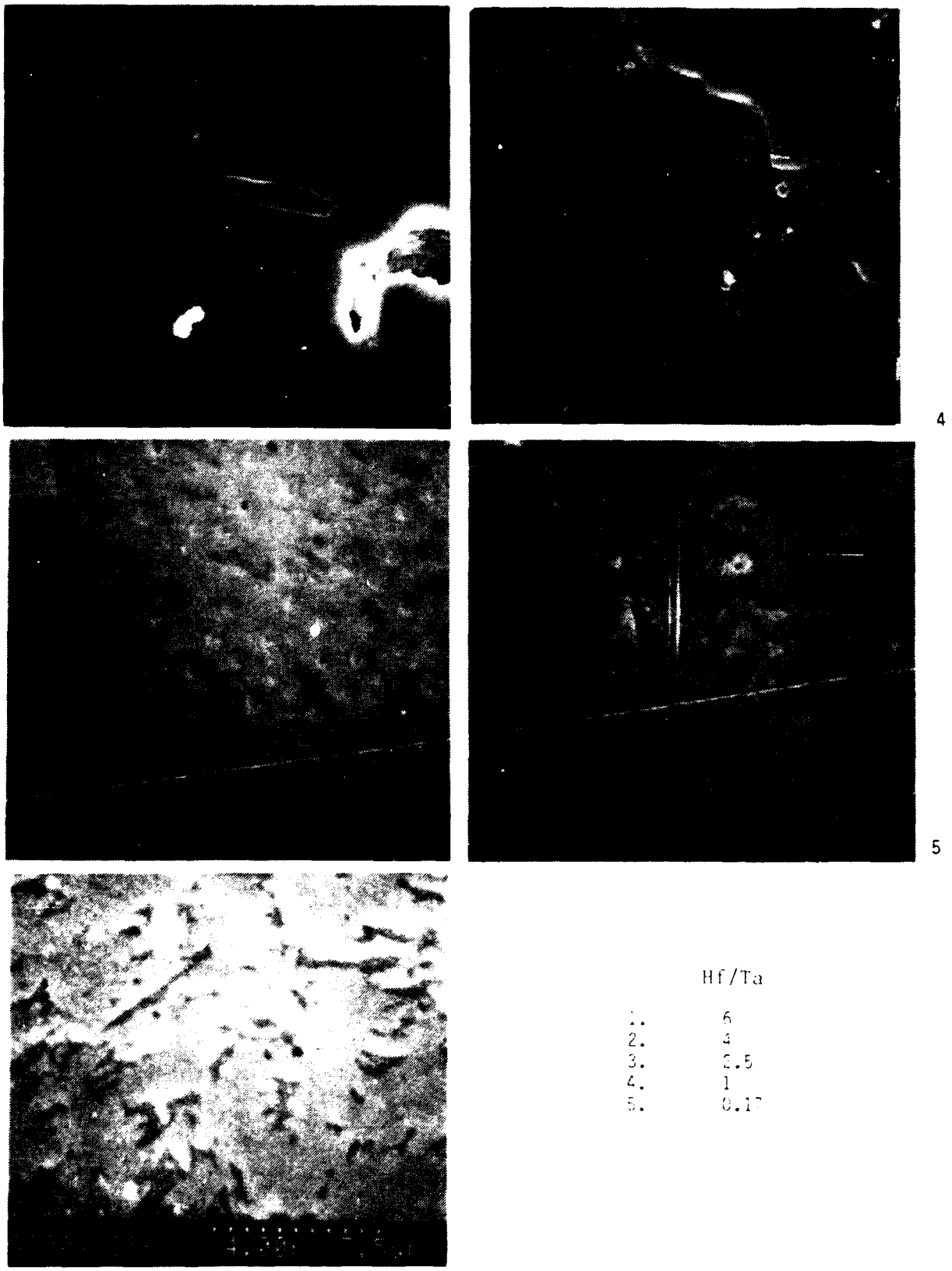

FIGURE 7. ELECTRON MICROGRAPHS (4000X)
OF QUENCHED LIQUIDS

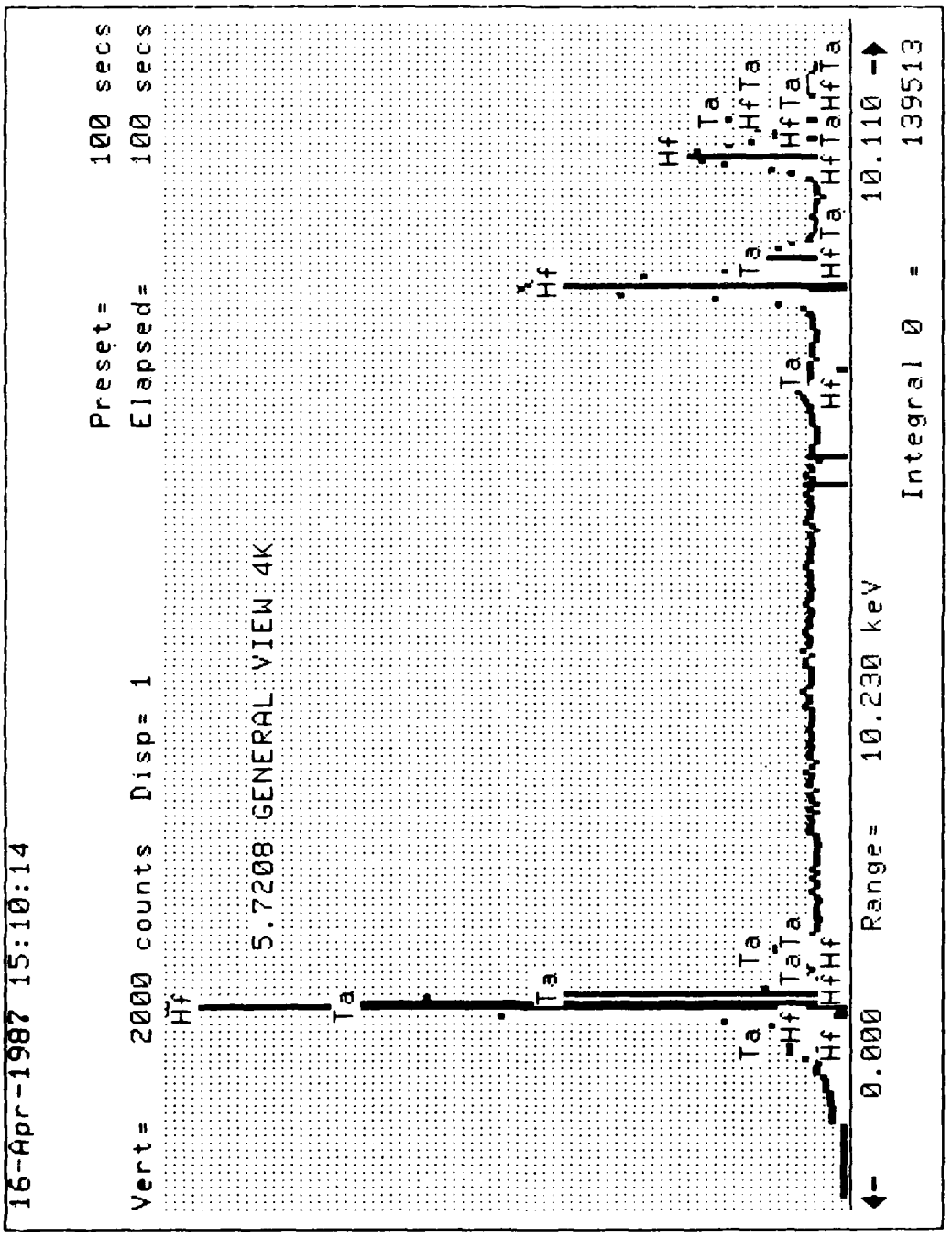

FIGURE 8. EDS SPECTRA OF Hf RICH MIXED OXIDE

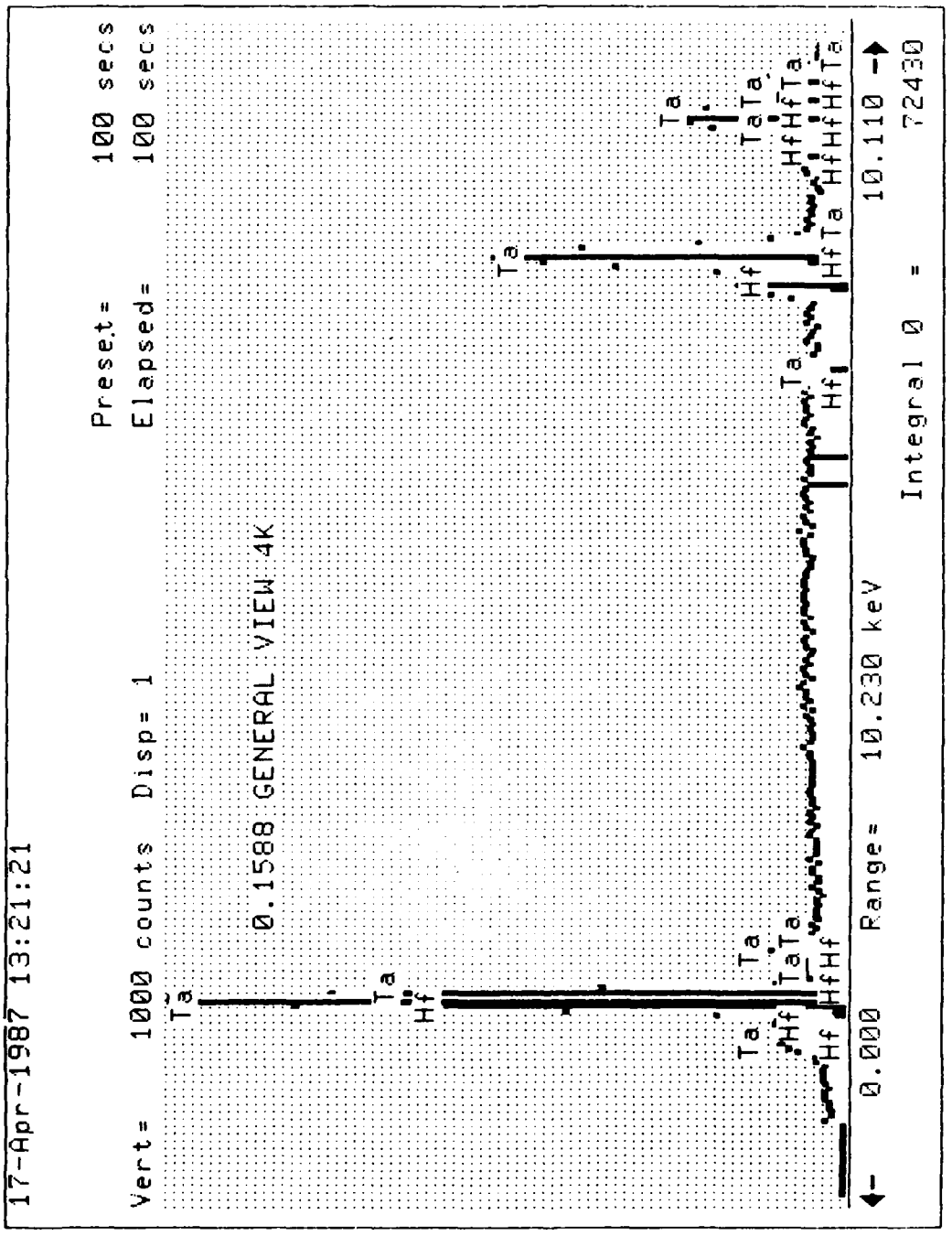

FIGURE 9. EDS SPECTRA OF Ta RICH MIXED OXIDE

count), the average composition of each sample was measured and plotted against the actual "as prepared" composition. Figure 10 shows the correlation of the measured (ZAF) atomic ratio to the actual values. The dashed line shows the "no error" correlation. As might be expected, the measured values are quite accurate near Hf=Ta.

At high concentrations, the software over-corrects for the presence of Ta indicating much higher Ta concentrations than actually exist. The reverse is true for high Ta compositions, where higher than real Hf concentrations are measured. In any case, by using this calibration curve, accurate Hf/Ta analyses are possible.

Each of the five compositions showing diphasic microstructure was quantitatively studied, with regard to the composition of the high Ta (softer, residual liquid) phase versus the Hf rich phase. The analytical results are summarized in Figure 11 where the composition of the two phases present is plotted versus the average composition of the sample. The dotted line shows the relationship which would occur if no phase separation occurred and a homogeneous solid solution formed. Instead, for example, at average Hf/Ta = 1.0, a residual liquid-like phase with Hf/Ta = 0.20 and a Hf rich phase with Hf/Ta = 2.7 form. At Hf/Ta = 6, the two phases have compositions Hf/Ta = 1.7 and Hf/Ta = 15.4. As shown, there is a dramatic shift in behavior between the composition at Hf/Ta = 4 compared to Hf/Ta = 2.5. It should be pointed out that for samples with ratios 4 and 6, the volume fraction of the Hf rich phase is relatively small. Thus, the primary phase present in the four compositions with ratios 1, 2.5, 4, 6 has a composition ratio of Hf/Ta in the range 2-3. This may explain some of the lack of variance observed in the x-ray diffraction patterns of Figure 6, but the correlation of the x-ray diffraction and phase analysis data would require much further study.

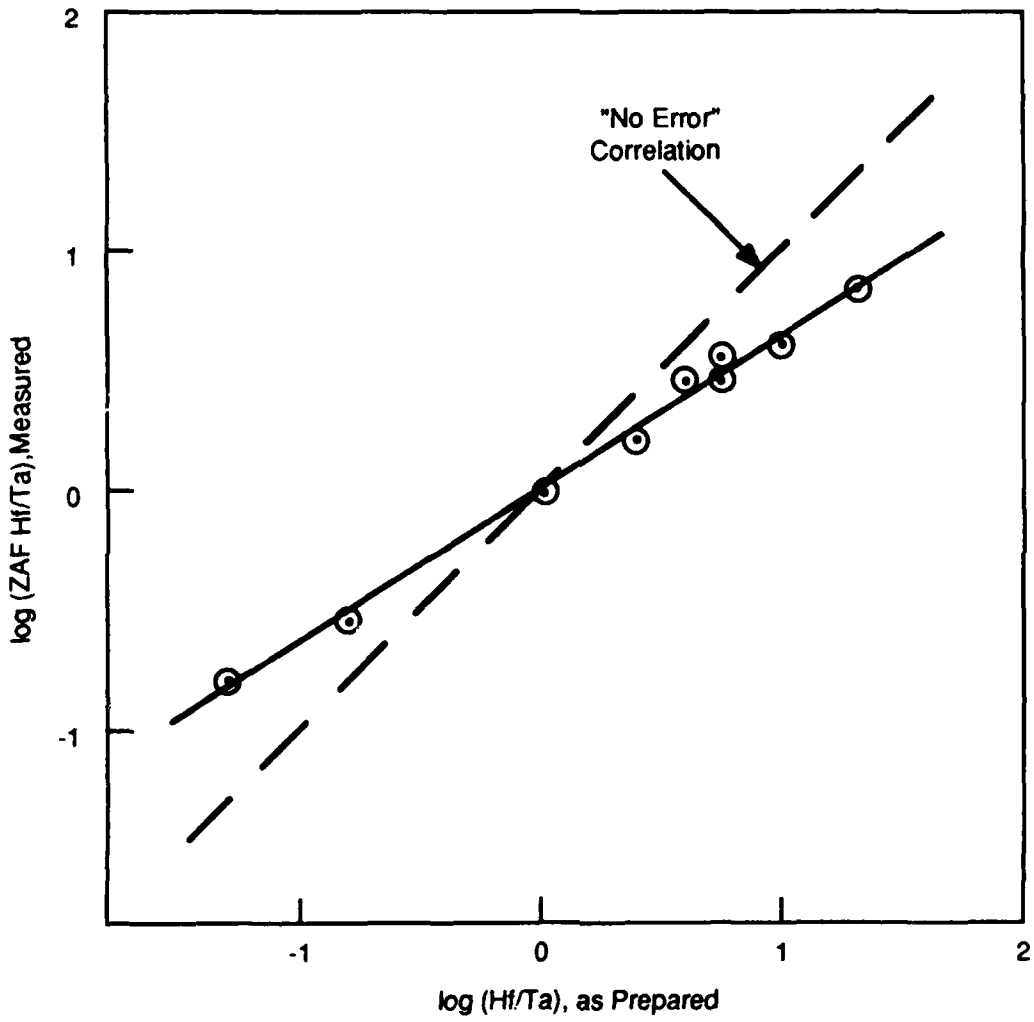

FIGURE 10. EDS CALIBRATION CURVE

The general result observed (Figure 11) is consistent with our expectations as a given composition cools through the liquid-solid diphasic region of the phase diagram, as shown schematically in Figure 12. As liquid of composition y cools to point x, a solid phase rich in HfO_2 can form, leaving a liquid phase rich in Ta_2O_5. The resulting mixture of solid phases is thus highly dependent on quench rates, the detailed shape of the liquidous-solidus curves and the underlying stability of the various crystalline phases which may form.

1900°C Quench

Pellets which had previously been furnace annealed at 1500°C were surface treated with the laser to temperatures about 1900°C. This involved moving the samples in the beam for a few minutes to repetitively heat sections of the surface to the 1900°C temperature. (The beam covered about 1/4 of the pellet area). The x-ray patterns obtained are shown in Figure 13. At Hf/Ta = 20, the pattern is essentially that of monoclinic HfO_2. At Hf/Ta = 1, the pattern is essentially pure $Hf_2Ta_2O_9$, with orthohombic symmetry. The four compositions in between are mixtures of these two phases. The relative proportions of each phase have not been estimated, but the trends are not as clear as observed at 1500°C, discussed in the next section.

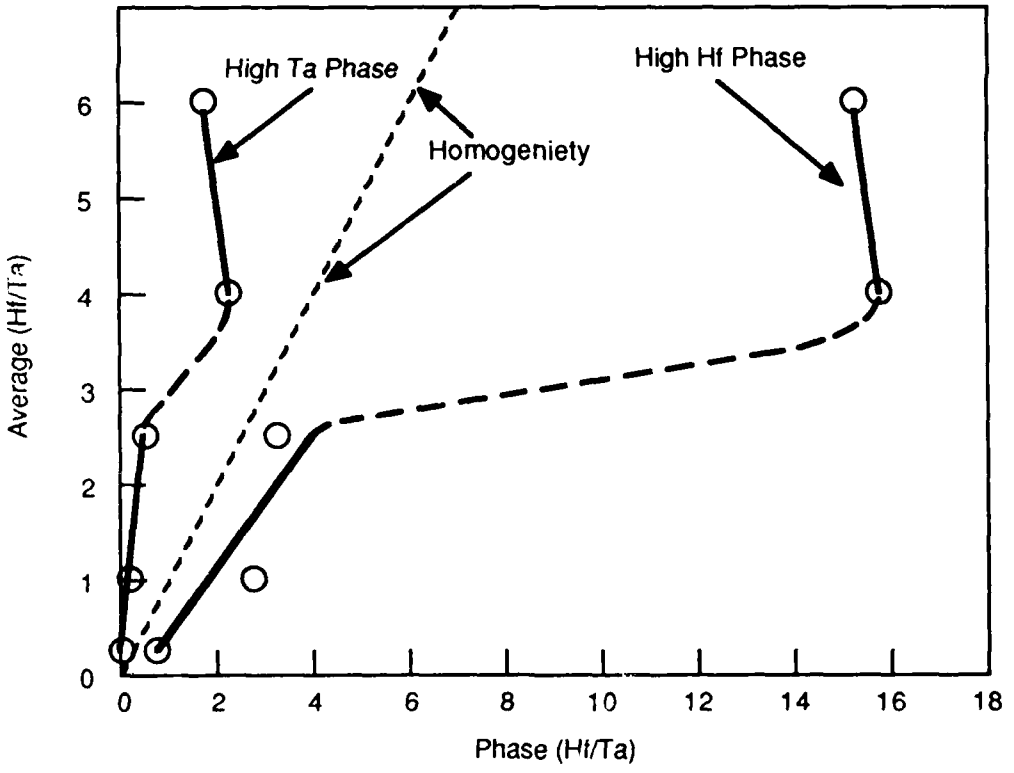

FIGURE 11. COMPOSITION OF TWO PHASES PRESENT IN QUENCHED LIQUIDS

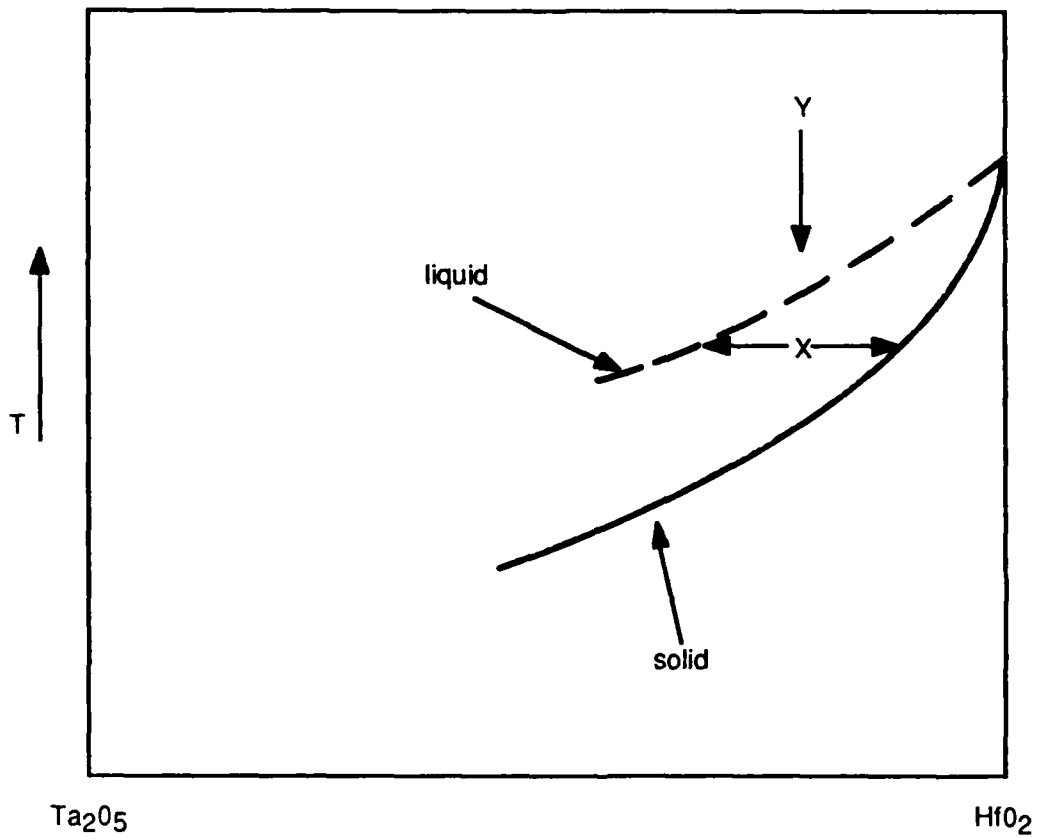

FIGURE 12. SCHEMATIC OF COOLING PATH

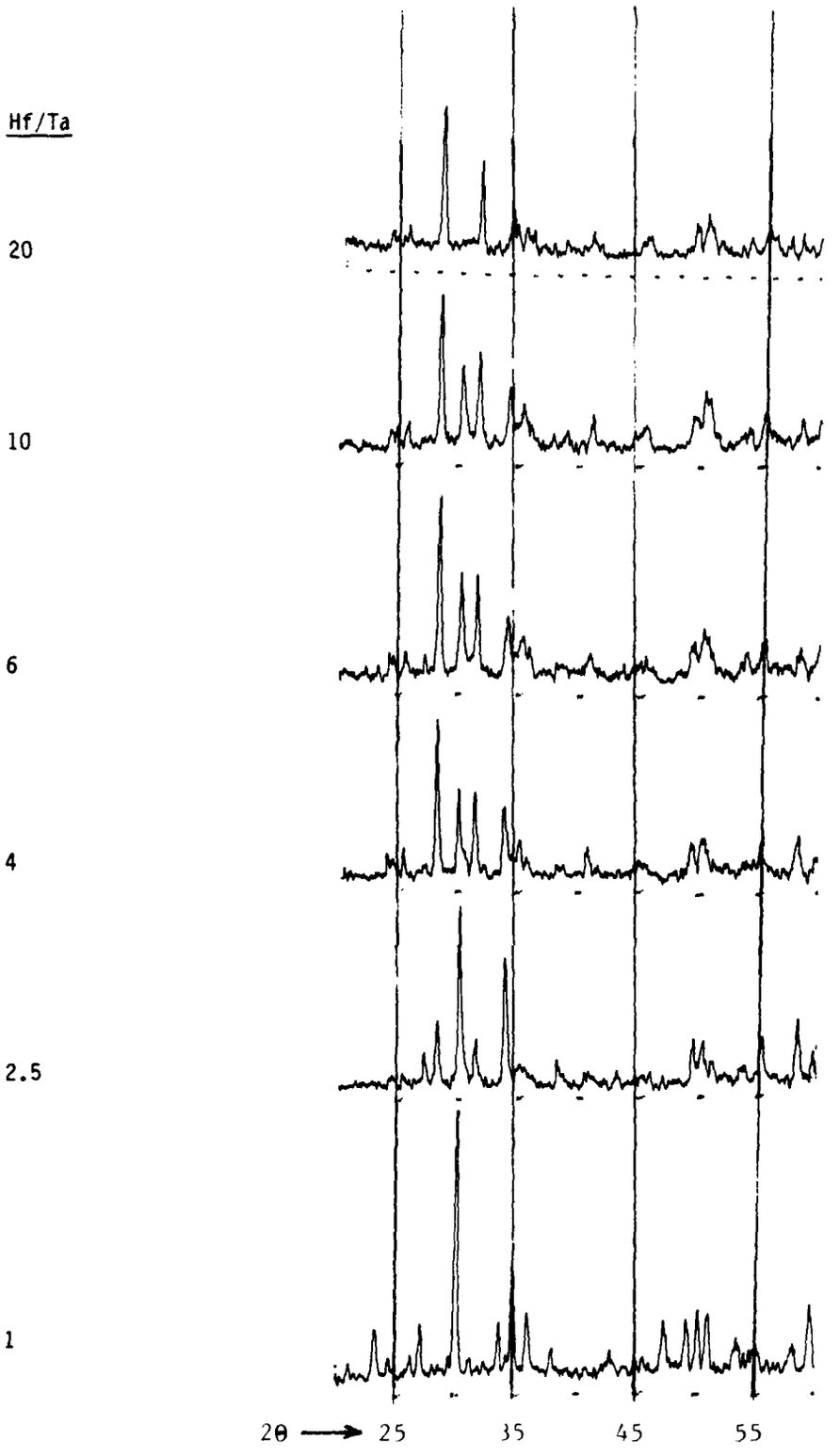

FIGURE 13. XRD TRACES OF SAMPLES QUENCHED FROM 1900°C

There were two objectives of this experiment. The first was to see if the primary phase observed after quenching melts (Figure 6) could be achieved by solid state reaction. There is no evidence this phase has formed. The second objective was to increase confidence that the information obtained at lower temperatures was not a result of incomplete reaction of the starting materials. Since the results support the 1500°C data, we conclude that the region from $Hf_2Ta_2O_9$ to HfO_2 is probably a diphasic mixture of these phases at least from 1500°C to near melting temperatures. Long term annealing experiments and preparation of the mixed oxides by better molecular mixing are required to prove this observation.

1500°C Quench

Samples quenched from 1500°C by removal from a box furnace gave the x-ray diffraction patterns shown in Figure 14. Near 30° (2θ), three strong diffraction peaks systematically change as the composition changes from Hf/Ta = 20 to Hf/Ta = 1. The peak at 30° (2θ) is from the $Hf_2Ta_2O_9$ phase. The peaks at 28 and 32° (2θ) are from monoclinic HfO_2. It is obvious one phase is simply replacing the other in a fairly systematic manner. A rough estimate of relative phase concentrations was made from the relative peak heights of the two phases. To do this, the two primary peaks for HfO_2 were summed and compared to the reflection from the $Hf_2Ta_2O_9$ phase. (The reason for this choice was simply that this ratio is approximately true in comparing the pure phases.) Table 1 shows the estimated concentrations of $Hf_2Ta_2O_9$ in each of the six compositions. The results are very close to the maximum concentrations calculated assuming simple diphasic mixtures exist. We conclude that is the case.

It was pointed out earlier that the diffraction pattern of the $Hf_2Ta_2O_9$ phase closely resembles the pattern reported by Spiridonov[1] for a series of mixed oxides with much higher Hf content. These workers also report a systematic shift of the position of the diffraction peaks as the composition changes. In these samples, we see no line shifts, suggesting that stoichiometry is fixed at $Hf_2Ta_2O_9$. Additional work is required to confirm this result.

1500°C Furnace Cool

A second series of samples was taken through an annealing cycle involving longer times at temperature and cooling at 20°C/minute. The x-ray diffraction results shown in Figure 15 are essentially the same as already discussed for samples quenched from 1500°C. This suggests that the formation of ordered phases reported by Spiridonov

1. Spiridonov, F.M. Mulenkova, M.N., Tsirelnikov, U.L., and Komissarova, L.N. "Intermediate Phases in the Hafnium dioxide-Tantalum pentoxide System," Russian J. of Inorg. Chem. 26 922 (1981)

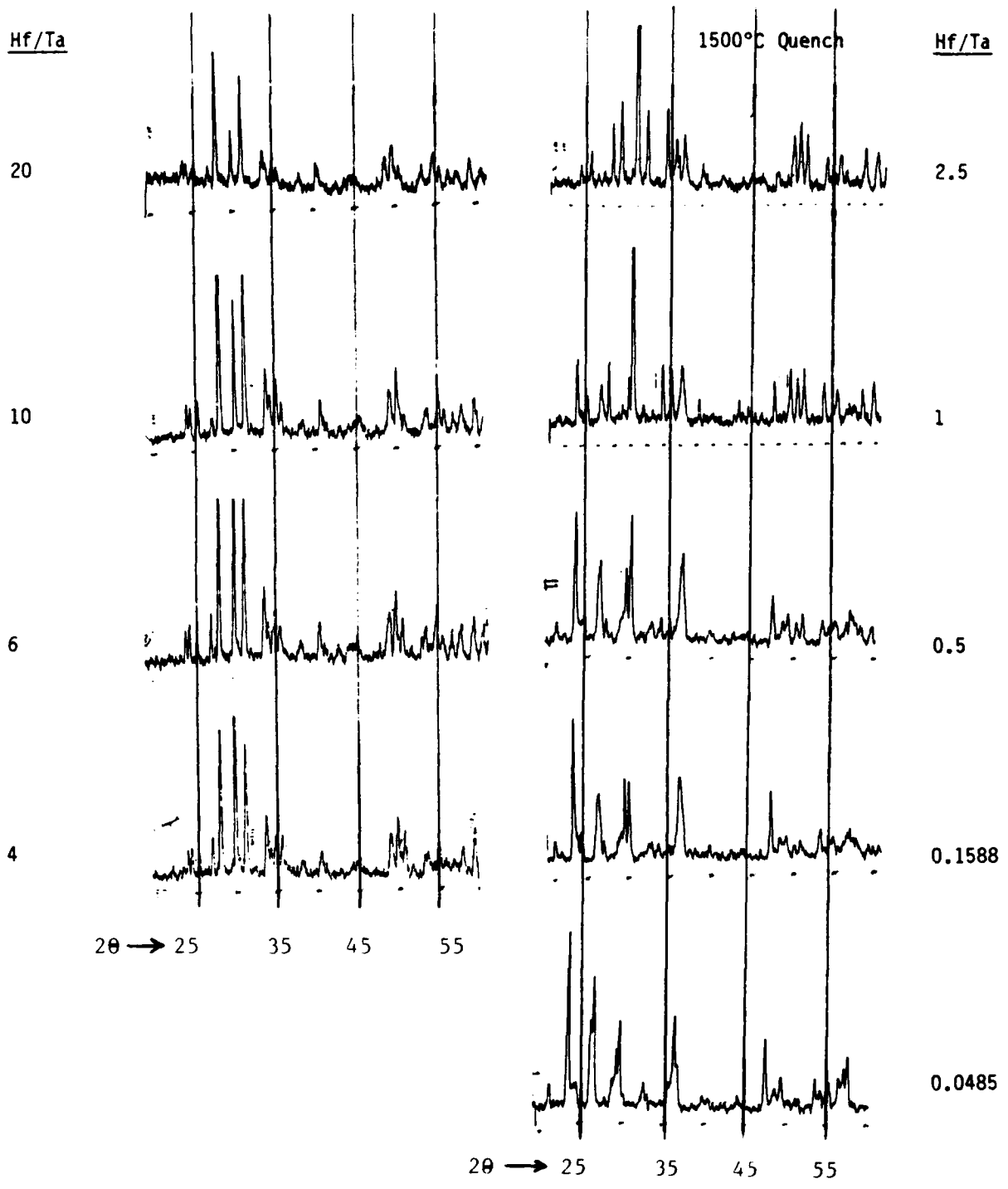

FIGURE 14. XRD TRACES OF SAMPLES QUENCHED FROM 1500°C

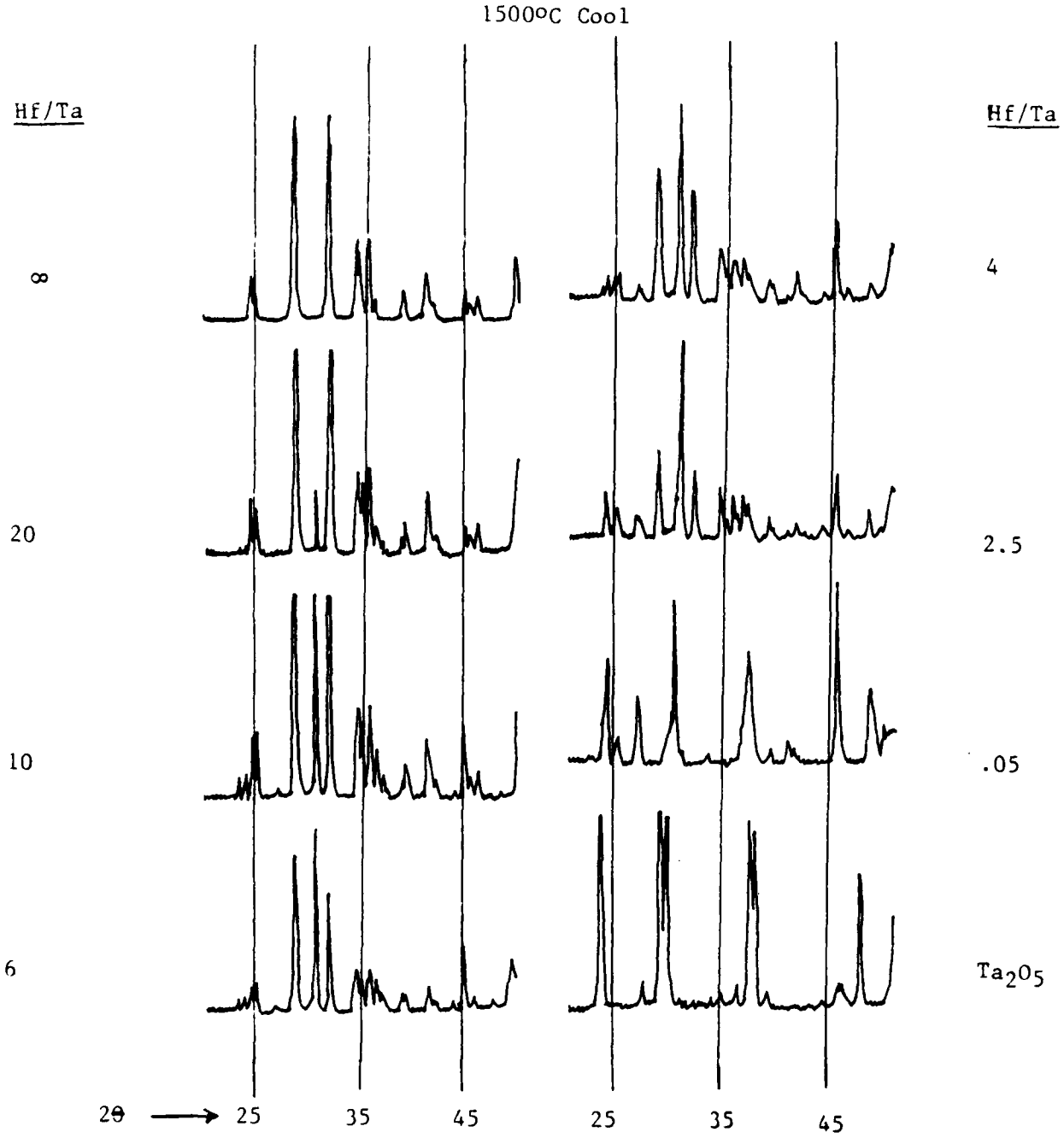

FIGURE 15. XRD TRACES OF SAMPLES COOLED FROM 1500°C AT 20°/MIN

TABLE 1. X-Ray Diffraction Determination of $Hf_2Ta_2O_9$ (Quenched From 1500°C)

	Relative Diffraction Intensities			
Hf/Ta	HfO_2*	$Hf_2Ta_2O_9$	$\%Hf_2Ta_2O_9$	$Hf_2Ta_2O_9$ Maximum % (Calculated)
∞	50	0	0	0
20	37	3	7	9.5
10	37	10	21	18
6	15	10	40	29
4	12	12	50	40
2.5	8	15	65	71
1.0	1	50	98	100

*Sum of Primary 2 Reflections

requires extended annealing at lower temperatures. It is also likely that the phases formed by approaching the annealing temperature from low temperature will be different from those observed by cooling from high temperatures unless very long annealing times are uses. Clearly, these issues would require work in addition to that so far completed, to be resolved.

DIFFUSION COUPLE STUDIES

An original intent of this project was to generate diffusion couple samples which could be studied on a microscale to directly understand phases formed as a function of composition, through the interface region. Several attempts were made to react polished pellets of the pure oxides at 1700°C, but contact (and pressure which could be applied) were not sufficient. It was found that a very good interface could be established by melting Ta_2O_5 onto a polished pellet of HfO_2. These could then be annealed to give the desired diffusion zone. We also recognized at this time that hafnium and tantalum x-ray fluorescence peaks are not resolved in the EDS system and concluded

(incorrectly) that quantitative analysis would probably be impossible. Hence, the diffusion couple approach was abandoned in favor of the quench studies reported in the previous sections. In retrospect, having now established that quantitative determination of the Hf/Ta ratio is possible, the diffusion couple approach is still highly attractive and would be a primary emphasis of any continuation of this study.

VOLATILITY

A few limited experiments were conducted to verify that tantalum oxide was not being vaporized rapidly from the molten materials, since this would strongly influence much of this study and might explain (for example) the unexpected x-ray diffraction similarity of a wide range of compositions quenched from the melt. Small beads of pure Ta_2O_5 and $Hf_2Ta_2O_9$ were maintained in the molten state at as high as 2300°C for various times up to about 5 minutes and periodically cooled and weighed. Within experimental error, no weight change was detected. Hence, under the conditions of this study it is believed no significant stoichometry changes occurred as a result of vaporization losses.

DIFFERENTIAL THERMAL ANALYSIS

Several experiments were made to determine whether any phase changes in the system might be observable by thermal analysis, although the equipment available is limited to 1500°C. The DSC traces are shown as Figures 16-20 for the following materials.

Figure 16	Pure Ta_2O_5 Fired at 1500°C
Figure 17	A Physical Mixture HfO_2/Ta_2O_5 = 0.95 (weight fraction)
Figure 18	Same as 17, but After Heat Treating the Mixture at 1500°C to Produce $Hf_2Ta_2O_9$
Figure 19	1500°C Fired Material with Weight Ratio at HfO_2/Ta_2O_5 = 0.238
Figure 20	1500°C Fired Material with Weight Ratio at HfO_2/Ta_2O_5 = 0.1589

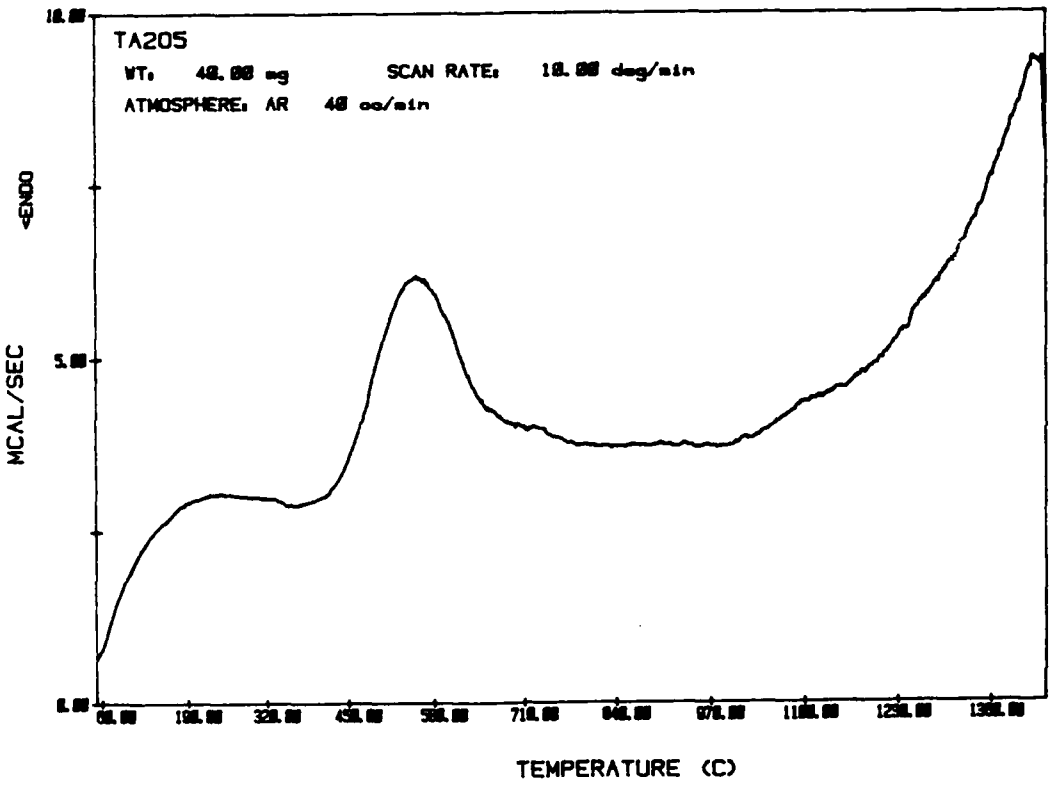

FIGURE 16. DTA TRACE FOR Ta_2O_5

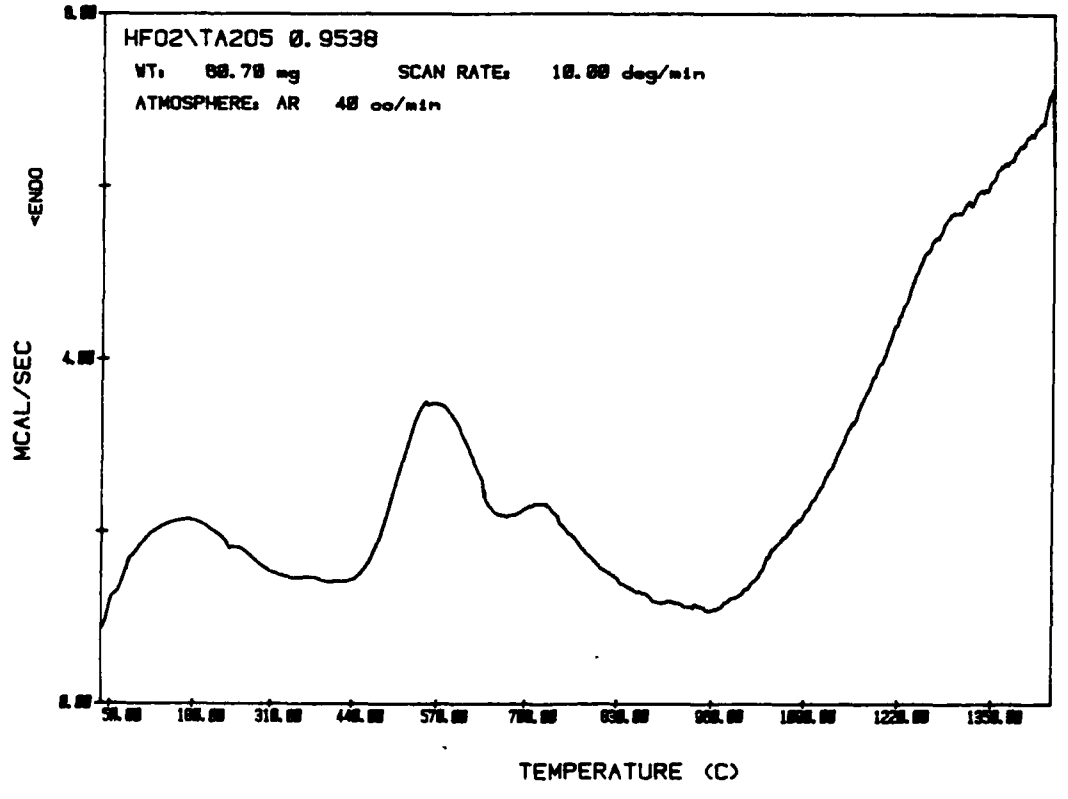

FIGURE 17. DTA TRACE FOR A PHYSICAL MIXTURE OF HfO_2/Ta_2O_5

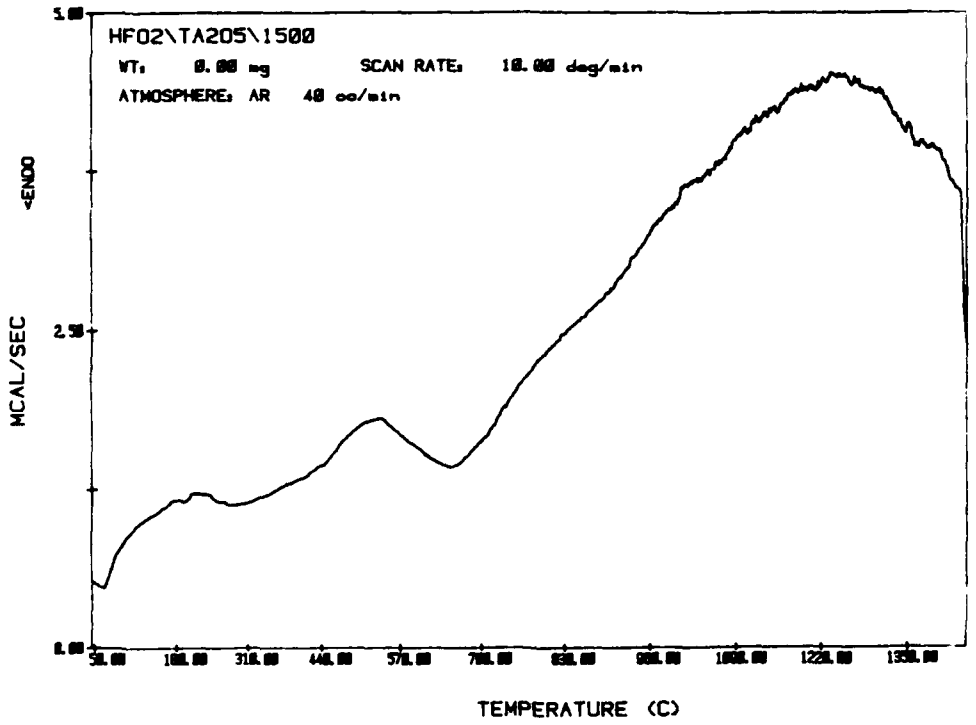

FIGURE 18. DTA TRACE FOR HfO_2/Ta_2O_9 AFTER HEAT TREATING THE MIXTURE AT 1500°C TO PRODUCE Hf_2Ta_2O9

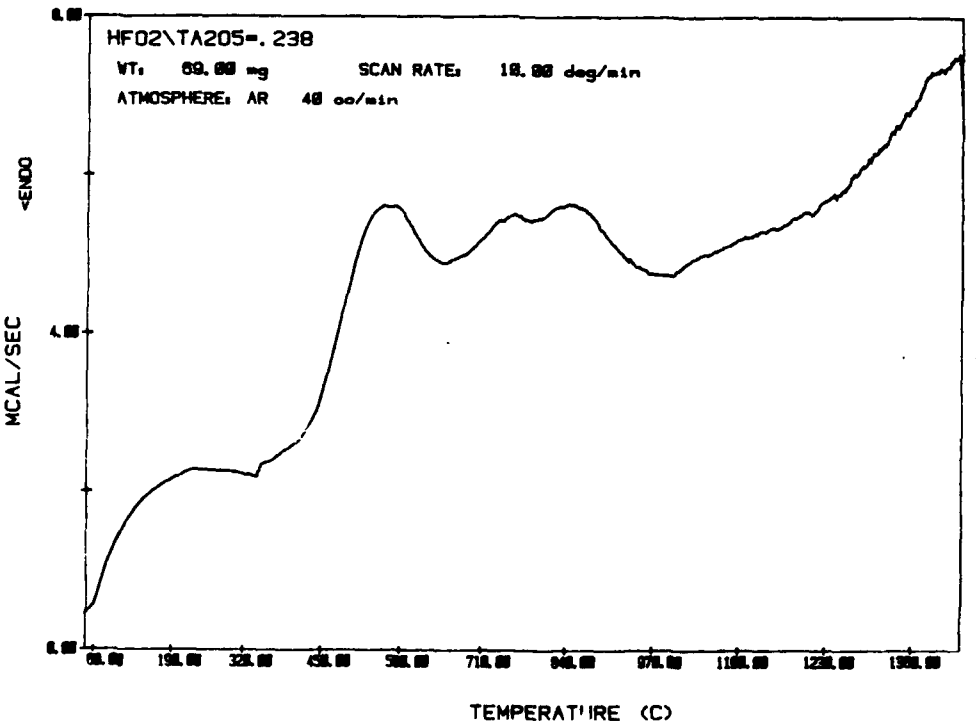

FIGURE 19. DTA TRACE FOR 1500° FIRED MATERIAL WITH WEIGHT RATIO AT HfO_2/Ta_2O_5 = 0.238

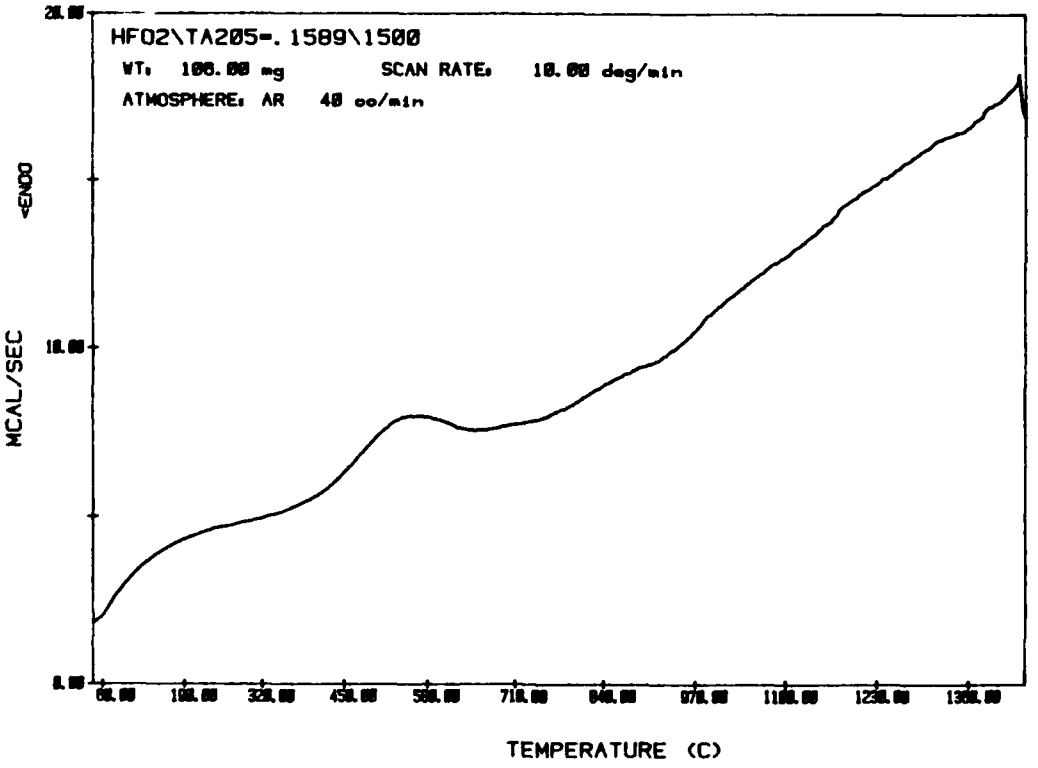

FIGURE 20. DTA TRACE FOR 1500°FIRED MATERIAL WITH WEIGHT RATIO AT HfO_2/Ta_2O_5 = 9.1589

It first should be noted that any exothermic reactions will be seen in the figures as positive shifts from the baseline. The baseline may also shift gradually as a result of the furnace/thermocouple configuration, having nothing to do with the sample or the reference material (Al_2O_3). This is especially true at the beginning of the heating cycle. Thus, in Figure 16, the broad exotherm at about 560°C is real and weak, broad exotherms near 700 and 1100°C may be real, but nothing else is of importance. In Figure 17, exotherms at 560°C, 750°C, 1080°C, and 1300°C are all meaningful. The other figures all show thermal excursions that could be studied. Comparing this kind of information to direct structural probes such as high temperature x-ray diffraction, would be required to develop the low temperature portion of the phase diagram. Because of the emphasis in this study on high temperature behavior, the DTA work was not continued even though it is clear much could be learned.

CONCLUSIONS

The primary conclusions of this Phase I study include the following:

- The melting temperature of mixed HfO_2-Ta_2O_5 oxides shows a rapid decrease from HfO_2 at 2800°C+ to temperatures at or below 2200°C with addition of less than 10 mole % Ta_2O_5.
- All Ta_2O_5 rich oxides melt in the range of 1800-2000°C.
- The maximum concentration of Ta_2O_5 dissolving in the monoclinic HfO_2 structure is less than or about 6 wt%, probably as a metastable solid solution.
- A new phase occurs in samples quenched from the liquid state. It dominates the mixed oxide range from Hf/Ta = 20 to Hf/Ta = 1. This phase appears to have a composition with Hf/Ta in the range 2-3.
- The phase $Hf_2Ta_2O_9$ appears to have an orthohombic crystal structure closely related to that reported for a series of more hafnium rich compounds. This phase is very stable with regard to possible reaction with HfO_2 to form mixed compounds of higher HfO_2 content. The high temperature region (above 1500°C) between HfO_2(ss) and this phase appears to remain as a diphasic mixture of these two compounds, in direct relation to the overall sample composition.

DISTRIBUTION

	Copies
Office of Naval Technology Attn: J. Kelly (OCNR 225) 800 N. Quincy Street Arlington, VA 22217-5000	1
Commander Naval Sea Systems Command Attn: M. Kinna (SEA 6205)) Washington, DC 20362	1
Commander Naval Weapons Center Attn: J. P. Newhouse (Code 3244) China Lake, CA 93555	1
Commander Naval Air Development Center Attn: W. G. Barker (Code 6063) Warminster, PA 18974	1
Defense Technical Information Center Cameron Station Alexandria, VA 22304-6145	12
Defense Advanced Research Projects Agency Attn: Dr. B. Wilcox Dr. F. Patten DARPA/DSO/MSD Arlington, VA 22209	1 1
AFWAL/FIBCB Attn: H. Croop Wright-Patterson AFB Dayton, OH 45433	1
AFWAL/MLBC Attn: L. S. Theibert S. L. Szaruga Wright-Patterson AFB Dayton, OH 45433	1 1
AFWAL/MLLM Attn: Dr. H. Graham Dr. R. Kearns Wright-Patterson AFB Dayton, OHB 45433	1 1
AFWAL/POPR Attn: LT M. Harter Wright-Patterson AFB Dayton, OH 45433	1
Library of Congress Attn: Gift and Exchange Division Washington, DC 20540	4
Acurex/Aerotherm Attn: Dr. J. Zimmer Aerospace Systems Division 485 Clyde Avenue Mountain View, CA 94042	1
Aerojet Strategic Propulsion Co. Attn: P. J. Marchol P.O. Box 15699C Sacramento, CA 95813	1
Aerospace Corporation Attn: Dr. R. Myers, M2-248 S. Evangelides, M2-248 P.O. Box 92957 Los Angeles, CA 90009	1 1
AIRCO Carbon Attn: M. Meiser Carbon Products Department P.O. Box 387 St. Marys, PA 15857	1

DISTRIBUTION (Cont.)

Copies

AIRCO TEMESCAL
Attn: W. K. Halnan 1
J. Egermeier 1
2850 Seventh Street
Berkeley, CA 94710

American Research Corporation of Virginia
Attn: Dr. H. P. Groger 1
642 First Street
P.O. Box 3406
Radford, VA 24143-3406

Applied Physics Laboratory
Johns Hopkins University
Attn: L. B. Weckesser (Group BBE) 1
R. Newman (Group BBE) 1
Dr. P. Waltrup (Group BBP) 1
B. Bargeron (Group BBP) 1
R. Benson (Group BBP) 1
Johns Hopkins Road
Laurel, MD 20707

Boeing Aerospace
Attn: M. Reissig, MS-82-23 1
Dr. A. Rugin, MS-82-97 1
P.O. Box 3999
Seattle, WA 98124

Ceramic Refractory Corporation
Attn: Dr. J. Hollander 1
Rutledge Road
Transfer, PA 16154

Fiber Materials, Inc.
Attn: Dr. D. Batha 1
Dr. R. Burns 1
Biddeford Industrial Park
Biddeford, ME 04005

Garrett Turbine Engine Company
Attn: J.Shemlie, MS-503-4Y 1
111 South 34th Street
Phoenix, AZ 85010

G. A. Technologies
Attn: Dr. J. Sheehan 1
P.O. Box 81608
San Diego, CA 92138

General Dynamics/Convair
Attn: W. Whatley, 43-6320 1
Dr. D. W. Stevens 44-6300 1
P.O. Box 85357
San Diego, CA 92138

General Dynamics
Attn: C. Bachman, 5984 1
P.O. Box 748
Ft. Worth, TX 76101

Grumman Aircraft Systems
Attn: Dr. J. Suarez, B10-25 1
Bethpage, NY 11714-3582

Hercules Aerospace
Attn: S. Lewis, MS X2B1 1
Magna, UT 84044

Hercules, Inc.
Attn: P. Bruno, MS X11M9 1
P.O. Box 98
Magna, UT 84044

Hughes Aircraft Company
Electro-Optical and Data Systems Group
Attn: J. Gibson
Gp Hd Ceramic Dept. 1
El Segundo, CA 90245

LTV Aerospace and Defense Company
Attn: D. L. Hunn, TH-85 1
Dr. D. W. Freitag, TH-85 1
P.O. Box 650003
Dallas, TX 75265-0003

Lockheed Missiles & Space Company
Attn: Dr. D. F. Baker, 0/93-30 B/204 1
3251 Hanover Street
Palo Alto, CA 94303-1187

Lockheed Missiles & Space Company
Attn: Dr. J. F. Creedon, 0/57-30 B/174 1
1111 Lockheed Way
Sunnyvale, CA 94088-3504

DISTRIBUTION (Cont.)

	Copies
Lockheed Missiles & Space Company Attn: A. Johnson, 62-92 B/564 1111 Lockheed Way Sunnyvale, CA 94086	1
McDonnell Douglas Corporation Attn: Dr. M. . Callahan P.O. Box 516 St. Louis, MO 63166	1
Manlabs, Inc. Attn: Dr. L. Kaufman 21 Erie St. Cambridge, MA 02139	1
Materials Sciences Corporation Attn: Dr. J. Kibler Gwynedd Plaza II Spring House, PA 19477	1
Morton Thiokol, Inc. Attn: A. Canfield, MS 284 P.O. Box 524 Brigham City, UT 84302	1
The Ohio State University Metallurgical Engineering Dept. Attn: Dr. G. R. St. Pierre 141A Fontana Labs 116 W. 19th Avenue Columbus, OH 43210-1179	1
Pratt & Whitney Attn: S. Singerman, MS707-26 Box 2691 West Palm Beach, FL 33402	1
Refractory Composites, Inc. Attn: J. W. Warren T. Pacquette 12220-A Rivera Rd. Whittier, CA 90606	1 1
Sandia National Laboratories Attn: A. B. Cox, Code 9142 Albuquerque, NM 87185	1
The Southern Illinois University at Carbondale Department of Mechanical Engineering Attn: Dr. J. Don Carbondale, IL 62901	1
Southern Research Institute Attn: S. Causey B. Johnson 2000 Ninth Avenue, South Birmingham, AL 35205	1 1
Techniweave, Inc. Attn: J. M. Crawford Mill & Front Streets P.O. Box 314 East Rochester, NH 03867	1
United Technologies Research Center Attn: Dr. R. Guile, MS 30A Dr. J. Strife East Hartford, CT 06108	1 1
Ultramet Attn: Dr. R. Tuffias 12173 Montague Street Pacoima, CA 91331	1
Internal Distribution:	
K06 (W. C. Lyons)	1
K201 (A. M. Morrison)	1
K205 (W.T. Messick)	1
K22	
K22 (J. Vamos)	1
K22 (M. Opeka)	5
R31 (C. Martin)	1
R31 (I. Talmy)	1
R35 (C.Blackmon)	1
G23 (R. Haag)	1
E231	2
E232	15